

# Ensemble of Convolutional Neural Networks Trained with Different Activation Functions

Gianluca Maguolo<sup>a</sup>, Loris Nanni<sup>a</sup>, and Stefano Ghidoni<sup>a</sup>

<sup>a</sup> *DEI, University of Padua, viale Gradenigo 6, Padua, Italy.*

## ABSTRACT

Activation functions play a vital role in the training of Convolutional Neural Networks. For this reason, to develop efficient and performing functions is a crucial problem in the deep learning community. Key to these approaches is to permit a reliable parameter learning, avoiding vanishing gradient problems. The goal of this work is to propose an ensemble of Convolutional Neural Networks trained using several different activation functions. Moreover, a novel activation function is here proposed for the first time.

Our aim is to improve the performance of Convolutional Neural Networks in small/medium size biomedical datasets. Our results clearly show that the proposed ensemble outperforms Convolutional Neural Networks trained with standard ReLU as activation function. The proposed ensemble outperforms with a p-value of 0.01 each tested stand-alone activation function; for reliable performance comparison we have tested our approach in more than 10 datasets, using two well-known Convolutional Neural Network: Vgg16 and ResNet50.

MATLAB code used here will be available at <https://github.com/LorisNanni>.

## 1. Introduction and State of the Art

Neural networks are one of the most popular tools in artificial intelligence. In recent years they became the state of the art technique in many fields like image classification [1], object detection [2], face recognition [3] and machine translation [4]. The first deep neural networks were trained using activation functions like the hyperbolic tangent or the sigmoid function. However, these functions saturate as the modulus of the input goes to infinity, while the gradients rapidly decrease, allowing only the training of shallow networks. In order to address these problems, in 2011 Glorot et al. [5] showed that deep networks can be efficiently trained using Rectified Linear Units (ReLU), an activation function which is the identity function if the input is positive and it is zero when it is negative [6]. Although this function is not differentiable, it outperformed the previous saturating activation functions, allowing AlexNet to win the ImageNet competition in 2012 [7]. Since ReLU was very effective, very simple and very fast to evaluate, in the following years, many deep learning researchers focused on finding ReLU-like activations with slightly different properties.

One example is Leaky ReLU [8], an activation function that is equal to ReLU for positive inputs (i.e.: the identity function) and it has a very small slope  $\alpha > 0$  for negative inputs,  $\alpha$  being a hyperparameter. In this way, the gradient of the function is never zero and it is less likely that the optimization process gets stucked in local minima. The same idea is the basis for Exponential Linear Units (ELU) [9]. ELU is once again equal to ReLU for positive inputs, but it exponentially decreases to a limit point  $\alpha$  as the input goes to minus infinity. This means that this activation has always positive gradient, but, unlike Leaky ReLU, saturates on its left side. Klambauer et al. proposed Scaled Exponential Linear Unit (SELU) [10], which is ELU multiplied by a constant  $\lambda$ . Their idea is to tune these hyperparameters in order to make SELU preserve the mean and the variance of its input features. This helps to mitigate the vanishing gradient problem and allows the authors to successfully train deep feed-forward networks.

Standard activation functions do not depend on any learnable parameters and the training of the network only modifies the weights and the biases. In 2015 He et al. [11] implemented Parametric ReLU (PReLU), which is a Leaky ReLU activation

function where the slope of the negative part is a learnable parameter. According to the authors, this idea was the key to reach super-human results in the ImageNet 2012 dataset. Since this method adds parameters to the network, this activation makes overfitting more likely, so it is suitable in particular for larger datasets. According to the authors, PReLU always outperforms non-learnable activations on the training set, but might fail to generalize on the test set. After that, many learnable activations with different shapes have been proposed [12,13]. In particular, Agostinelli et al. [12] proposed a piecewise linear activation that they called Adaptive Piecewise Linear Unit (APLU), whose slopes and points of non differentiability are learnt at training time. This method is the most similar to the one that we propose here.

Learnable activations can also be defined using multiple fixed activations as their starting point. Manessi and Rozza [14] created a new learnable activation function by learning an affine combination of tanh, ReLU and the identity function. More recently, Ramachandran et al. [15] proposed the Swish activation function  $f(x) = x\sigma(x)$  where  $\sigma(\cdot)$  is the sigmoid activation and  $\beta$  is a parameter that can optionally be learnable. The authors found this activation function using reinforcement learning. They created a network that tried to create different activation functions with a reward related to the performance of the activation function chosen. They used very simple activations as building blocks that their network could use to generate more complex activations. According to them, the best performing function was the Swish activation. In the reinforcement learning framework, only standard activations were considered. This means that the Swish activation was found keeping the parameter  $\beta$  fixed. However, in their tests the activation performed better if it was set to be learnable.

In this paper we propose a piecewise linear activation function which is the sum of PReLU and multiple Mexican hat functions: we named our approach Mexican ReLU (MeLU). It has a number of parameters that ranges from zero to infinity. In our case, the total number of parameters is a hyperparameter. It is built to have desirable properties that can improve the representation power of the network and help the network to reach better minima. First of all, if the number of parameters goes to infinity, it can approximate every continuous function  $f$  on a compact set. Moreover, it does not saturate in any direction and its gradient is almost never flat. Finally, modifying a parameter changes the activation only on a small interval, making the optimization process simpler.

The most important results of this work are the following:

- We compare several activation functions, using two different Convolutional Neural Networks (CNN), in more than ten small/medium size biomedical dataset. The CNN chosen for our tests are the Vgg16 [16] and ResNet50 [1].
- We show that an ensemble of activation functions (AF) strongly outperforms each AF singularly considered.
- We propose a new activation function.

The rest of the paper is organized as follows. In Section 2 we describe the most popular activation functions in the literature. In Section 3 we introduce MeLU and present its most important properties. In Section 4 we evaluate our activation on many different datasets, and we compare it with other methods presented in Section 2. Conclusions and take-home messages are summarized in Section 5.

## 2. Activation functions for CNNs

In this section we present some of the best performing activation functions proposed in the literature. We compared these functions by substituting them into two well-known CNNs, ResNet50 and VGG16, pre-trained on ImageNet.

ResNet50 is a CNN whose main features are called skip connections [1]. The difference with the usual building block of a standard CNN, namely a convolution followed by an activation, is that in a skip connection the input of a block is summed to its output. This should help the gradient flow.

VGG16 is a CNN whose blocks are made of small stacked convolutional filters [16]. It has been shown that they have the same effect of larger convolutional filters, but they use less parameters.

### 2.1. Rectified Linear Units

Rectified Linear Unit (ReLU) was first introduced in [6]. It is defined as

$$y_i = f(x_i) = \begin{cases} 0, & x_i < 0 \\ x_i, & x_i \geq 0 \end{cases}$$

Its gradient is

$$\frac{dy_i}{dx_i} = f'(x_i) = \begin{cases} 0, & x_i < 0 \\ 1, & x_i \geq 0 \end{cases}$$

### 2.2. Leaky ReLU

Leaky ReLU was first introduced in [8]. It is defined as

$$y_i = f(x_i) = \begin{cases} ax_i, & x_i < 0 \\ x_i, & x_i \geq 0 \end{cases}$$

Where  $a$  is a small real number. With respect to ReLU, this function has the advantage that there is no point where the gradient is null, helping the optimization process. Its gradient is

$$\frac{dy_i}{dx_i} = f'(x_i) = \begin{cases} a, & x_i < 0 \\ 1, & x_i \geq 0 \end{cases}$$

In the experiments we used  $a = 0.01$ .

### 2.3. ELU

Exponential Linear Unit (ELU) was firstly introduced in [9]. It is defined as

$$y_i = f(x_i) = \begin{cases} a(\exp(x_i) - 1), & x_i < 0 \\ x_i, & x_i \geq 0 \end{cases}$$

Where  $a$  is a real number. Like Leaky ReLU the gradient of this function is always positive. Besides it has the advantage of being differentiable. It also has the property of being bounded from below by  $-a$ . Its gradient is

$$\frac{dy_i}{dx_i} = f'(x_i) = \begin{cases} a \exp(x_i), & x_i < 0 \\ 1, & x_i \geq 0 \end{cases}$$

In the experiments we set  $a = 1$ .

### 2.4. SELU

Scaled Exponential Linear Unit (SELU) was firstly introduced in [10]. It is defined as

$$y_i = f(x_i) = \begin{cases} sa(\exp x_i - 1), & x_i < 0 \\ sx_i, & x_i \geq 0 \end{cases}$$

where  $a, s$  are real numbers. This function is basically ELU multiplied by an additional parameter. It was created in the context of feed-forward networks to avoid the problem of gradient vanishing or explosion. Klambauer sets the parameters  $a = 1.6733$  and  $s = 1.0507$  because this choice of the parameters allows SELU to map a random variable of null mean and unit variance in a random variable with null mean and unit variance. Its gradient is given by

$$\frac{dy_i}{dx_i} = f'(x_i) = \begin{cases} sa \exp(x_i), & x_i < 0 \\ s, & x_i \geq 0 \end{cases}$$

### 2.5. PReLU

Parametric ReLU was firstly introduced in [11]. It is defined as

$$y_i = f(x_i) = \begin{cases} a_c x_i, & x_i < 0 \\ x_i, & x_i \geq 0 \end{cases}$$

where  $a_c$  are real numbers that are different for every channel of the input. The big difference between this function and Leaky ReLU is that the parameters  $a_c$  are learnable. Its gradient is given by

$$\frac{dy_i}{dx_i} = f'(x_i) = \begin{cases} a_c, & x_i < 0 \\ 1, & x_i \geq 0 \end{cases}$$

$$\frac{dy_i}{da_c} = \begin{cases} x_i, & x_i < 0 \\ 0, & x_i \geq 0 \end{cases}$$

The slopes of the left hand sides are all initialized at 0.

### 2.6. S-Shaped ReLU (SReLU)

S-Shaped ReLU was firstly introduced in [17]. It is defined as

$$y_i = f(x_i) = \begin{cases} t^l + a^l(x_i - t^l), & x_i < t^l \\ x_i, & t^l \leq x_i \leq t^r \\ t^r + a^r(x_i - t^r), & x_i > t^r \end{cases}$$

Where  $t^l, t^r, a^l, a^r$  are learnable real numbers. This function has a very large representation power thanks to the high number of parameters. Its gradient is

$$\frac{dy_i}{dx_i} = f'(x_i) = \begin{cases} a^l, & x_i < t^l \\ 1, & t^l \leq x_i \leq t^r \\ a^r, & x_i > t^r \end{cases}$$

$$\frac{dy_i}{da^l} = \begin{cases} x_i - t^l, & x_i < t^l \\ 0, & x_i \geq t^l \end{cases}$$

$$\frac{dy_i}{dt^l} = \begin{cases} -a^l, & x_i < t^l \\ 0, & x_i \geq t^l \end{cases}$$

The learnable parameters are initialized as  $a^l = 0, t^l = 0, a^r = 1, t^r = \text{maxInput}$ , where  $\text{maxInput}$  is a hyperparameter.

## 2.7. APLU

Adaptive Piecewise Linear Unit (APLU) was introduced in [12]. It is defined as

$$y_i = \text{ReLU}(x_i) + \sum_{c=1}^n a_c \min(0, -x_i + b_c)$$

Where  $a_c, b_c$  are real numbers that are different for every channel of the input. This function is piecewise linear and it can approximate any continuous function on a compact set, for a suitable choice of the parameters, as  $n$  goes to infinity. The gradient of APLU is given by the sum of the gradients of ReLU and of the functions contained in the sum. The gradients of APLU with respect to the parameters are

$$\frac{df(x, a)}{da_c} = \begin{cases} -x + b_c, & x < b_c \\ 0, & x \geq b_c \end{cases}$$

$$\frac{df(x, a)}{db_c} = \begin{cases} -a_c, & x < b_c \\ 0, & x \geq b_c \end{cases}$$

The parameters  $a_c$  were initialized at 0, while the points were initialized at random. Besides, we added a  $0.001 L^2$ -penalty on the norm of the parameters  $a_c$ , which means that we added an additional term to the loss function which is

$$L^{\text{reg}} = \sum_{c=1}^n |a_c|^2$$

We also used a relative learning rate for these parameters that was  $\text{maxInput}$  times smaller than the one used for the rest of the network. This means that, if  $\lambda$  is the global learning rate, the learning rate  $\lambda^*$  of the parameters  $a_c$  is given by

$$\lambda^* = \frac{\lambda}{\text{maxInput}}$$

## 3. Mexican ReLU

In order to define Mexican ReLU (MeLU), let

$$\phi^{a,\lambda}(x) = \max(\lambda - |x - a|, 0)$$

be a ‘‘Mexican hat type’’ function, where  $a, \lambda$  are real numbers. The name comes from the fact that this function is null when  $|x - a| >$

$\lambda$  and it constantly increases with a derivative of 1 between  $a - \lambda$  and  $a$  and decreases with a derivative of minus 1 between  $a$  and  $a + \lambda$ . If one draws it, it has the shape of a Mexican hat. We are aware that the term Mexican hat refers to a famous wavelet in the field of computer vision, we chose to call  $\phi^{a,\lambda}(x)$  ‘‘Mexican hat type’’ because its shape is similar to the shape of the wavelet. These functions are the building blocks of MeLU. MeLU is defined as

$$y_i = \text{MeLU}(x_i) = \text{PReLU}^{c_0}(x_i) + \sum_{j=1}^k c_j \phi^{a_j, \lambda_j}(x_i)$$

For each channel of the hidden layer. The parameters  $c_j$  are learnable,  $a_j, \lambda_j$  are fixed and they are chosen recursively.  $c_0$  is the vector of parameters of PReLU. First of all, we set the parameter  $\text{maxInput}$ . The first Mexican hat function has its maximum in  $2 \cdot \text{maxInput}$  and it is equal to zero in 0 and  $4 \cdot \text{maxInput}$ . The next two functions are chosen to be zero outside, respectively, the interval  $[0, 2 \cdot \text{maxInput}]$  and  $[2 \cdot \text{maxInput}, 4 \cdot \text{maxInput}]$ , and imposing that they have their maximum in  $\text{maxInput}$  and  $3 \cdot \text{maxInput}$ .

Table 1. Fixed parameters of MeLU with  $\text{maxInput} = 256$ .

j	1	2	3	4	5	6	7
$a_j$	512	256	768	128	384	640	896
$\lambda_j$	512	256	256	128	128	128	128

We now show some properties of MeLU. The Mexican hat functions are continuous and piecewise differentiable, so MeLU inherits these properties. If all the  $c_i$  are initialized at zero, MeLU coincides with ReLU. This helps transfer learning when we substitute MeLU in a network pretrained with ReLU. The same holds for networks trained with Leaky ReLU or PReLU. Moreover, the Mexican hat functions are a Hilbert basis on a compact set with the  $L^2$  norm, hence they can approximate every function in  $L^2([0, 1024])$  as  $k$  goes to infinity.

It is worth noting that the structure of a hidden layer is  $f(Ah + b)$ , where  $h$  is the input of the hidden layer,  $A$  is the weight matrix,  $b$  is the bias and  $f$  is the activation. If we consider the joint optimization of the weights, the bias and the activation parameters, we see that we can approximate any continuous function on a compact set. Consider an interval  $I$  and let  $g$  be a function on that interval. We can approximate  $g$  using MeLU by simply choosing  $A, b$  to map  $I$  into  $[0, 1024]$  falling in the previous case, which is the approximation on a compact set.

Let us now focus on the relationship between MeLU and the other activations in the literature. It is clear that MeLU extends ReLU, Leaky ReLU and PReLU. Since it has more parameters, it has a higher representation power, but it might overfit easily. The most similar activations to MeLU in the literature are S-shaped ReLU and APLU. S-shaped ReLU is somehow the dual of MeLU: S-shaped ReLU divides the real line into two half lines and an interval and changes the slope of the activation on the two half lines. Conversely, most of the basis functions of MeLU have a limited support.

APLU and MeLU look very similar. Indeed, they can approximate the same set of functions: piecewise linear functions which are equal to the identity for  $x$  large enough. However, they do it in a very different way. For the right choice of the parameters, APLU can be equal to any piecewise linear function because the points of non-differentiability are learnable, while MeLU can represent every piecewise linear function only exploiting the joint optimization of the weights matrix and the biases. This means that MeLU adds to a network one half of the parameters of APLU and has the same representation power. The second difference between

the two functions is in the gradients. In optimizing a neural network there are two important factors: the output of every hidden layer and the gradient of that output with respect to the parameters. The gradients of MeLU with respect to the parameters are the Mexican hat functions. The gradients of APLU are computed in Section 2.7. It is clear that they are very different. The strong point of the solution we propose is its superior performance at the optimization stage. Without loss of generality, suppose that at a certain point in the training process  $b_1 > b_2 > \dots > b_n$ . Suppose now that it would be optimal for the network to modify the activation function between  $b_1$  and  $b_2$ . The only parameters whose gradients are not null in that interval are  $a_1$  and  $b_1$ , so changing them would be optimal. However, changing  $a_1$  has a very small effect near  $b_1$ , since the modulus of its gradient is the distance between  $x$  and  $b_1$ . The only option left would be changing  $b_1$ . However, even this option is not very good, since this would change the function even where it is not needed, since the support of the gradient is unbounded. This means that the optimization process might be very inefficient. Conversely, in the same situation, MeLU changes the activation exactly where it is needed, making the optimization easier. In the figure below, we can see the difference between the basis functions of MeLU and APLU. This might be the reason why the coefficients in APLU must be regularized with an  $L^2$  penalty and benefit from a low learning rate, while MeLU does not need any regularization.

In our experiments we set  $k = 4,8$ . The learnable parameters are initialized to zero, so the activation is initialized to be ReLU. This helps the training at the very beginning, exploiting all the nice properties of ReLU. For example, MeLU is convex for many iterations at the beginning of the training.

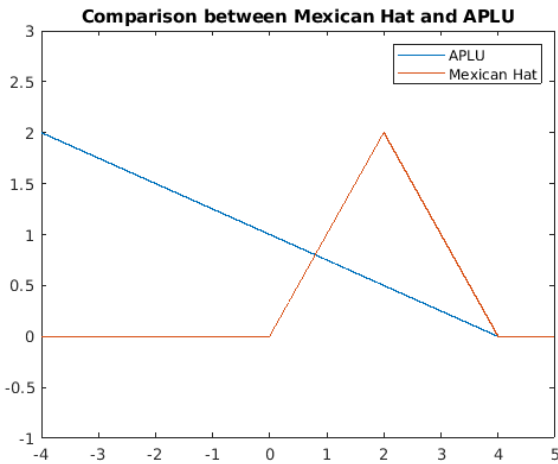


Figure 1. Partial derivatives of MeLU and APLU

#### 4. Experimental Results

We tested our novel activation function using the CNNs detailed in the previous section on a heterogeneous selection of publicly

available datasets. In detail, the datasets (summarized in Table 2) are:

- CH: the CHINESE HAMSTER OVARY CELLS dataset [18],
- HE: the 2D HELA dataset [18],
- LO: the Locate Endogenous dataset [19],
- TR: the LOCATE TRANSFECTED dataset [19],
- RN: the FLY CELL dataset [20]
- MA: Muscle aging [20]. This dataset includes images of *C. elegans* muscles at 4 ages (that represent the four classes).
- TB: Terminal bulb aging [20] dataset of images of *C. elegans* terminal bulb at 7 ages, constituting the 7 classes.
- LY: Lymphoma dataset [20].
- LG: Liver gender [20]. This dataset shows liver tissue sections from 6-month male and female mice on a caloric restriction diet, the 2 classes being male vs female.
- LA: Liver aging [20]. This dataset shows liver tissue sections from female mice on ad-libitum diet of 4 ages (the 4 classes).
- CO: histological images of human colorectal cancer [21].
- BGR: breast grading carcinoma [22].
- LAR: Laryngeal dataset [23]

Table 2  
Descriptive Summary of the Datasets: the number of classes (#C), number of samples (#S)

Dataset	#C	#S	URL for Download
CH	5	327	<a href="http://ome.grc.nia.nih.gov/iicbu2008/hela/index.html#cho">http://ome.grc.nia.nih.gov/iicbu2008/hela/index.html#cho</a>
HE	10	862	<a href="http://ome.grc.nia.nih.gov/iicbu2008/hela/index.html">http://ome.grc.nia.nih.gov/iicbu2008/hela/index.html</a>
LO	10	502	<a href="http://locate.imb.uq.edu.au/downloads.shtml">http://locate.imb.uq.edu.au/downloads.shtml</a>
TR	11	553	<a href="http://locate.imb.uq.edu.au/downloads.shtml">http://locate.imb.uq.edu.au/downloads.shtml</a>
RN	10	200	<a href="http://ome.grc.nia.nih.gov/iicbu2008/rnai/index.html">http://ome.grc.nia.nih.gov/iicbu2008/rnai/index.html</a>
TB	7	970	<a href="https://ome.grc.nia.nih.gov/iicbu2008">https://ome.grc.nia.nih.gov/iicbu2008</a>
LY	3	375	<a href="https://ome.grc.nia.nih.gov/iicbu2008">https://ome.grc.nia.nih.gov/iicbu2008</a>
MA	4	237	<a href="https://ome.grc.nia.nih.gov/iicbu2008">https://ome.grc.nia.nih.gov/iicbu2008</a>
LG	2	265	<a href="https://ome.grc.nia.nih.gov/iicbu2008">https://ome.grc.nia.nih.gov/iicbu2008</a>
LA	4	529	<a href="https://ome.grc.nia.nih.gov/iicbu2008">https://ome.grc.nia.nih.gov/iicbu2008</a>
CO	8	500	<a href="https://zenodo.org/record/53169#.WaXjW8hJaU0m">https://zenodo.org/record/53169#.WaXjW8hJaU0m</a>
BGR	3	300	<a href="https://zenodo.org/record/834910#.Wp1bQ-jOWUI">https://zenodo.org/record/834910#.Wp1bQ-jOWUI</a>
LAR	3	1320	<a href="https://zenodo.org/record/1003200#.WdeQcnBx0nQ">https://zenodo.org/record/1003200#.WdeQcnBx0nQ</a>

Table 3. Performance obtained using ResNet.

	Activation	CH	HE	LO	TR	RN	TB	LY	MA	LG	LA	CO	BG	LAR	Avg
Resnet50	MeLU (k=8)	92.92	86.40	91.80	82.91	25.50	56.29	67.47	76.25	91.00	82.48	94.82	89.67	88.79	78.94
MaxInput=1	Leaky ReLU	89.23	87.09	92.80	84.18	34.00	57.11	70.93	79.17	93.67	82.48	95.66	90.33	87.27	80.30
	ELU	90.15	86.74	94.00	85.82	48.00	60.82	65.33	85.00	<b>96.00</b>	90.10	95.14	89.33	<b>89.92</b>	82.79
	MeLU (k=4)	91.08	85.35	92.80	84.91	27.50	55.36	68.53	77.08	90.00	79.43	95.34	89.33	87.20	78.76
	PReLU	92.00	85.35	91.40	81.64	33.50	57.11	68.80	76.25	88.33	82.10	95.68	88.67	89.55	79.26
	SReLU	91.38	85.58	92.60	83.27	30.00	55.88	69.33	75.00	88.00	82.10	95.66	89.00	89.47	79.02
	APLU	92.31	87.09	93.20	80.91	25.00	54.12	67.20	76.67	93.00	82.67	95.46	90.33	88.86	78.98
	ReLU	93.54	<b>89.88</b>	95.60	<b>90.00</b>	55.00	58.45	<b>77.87</b>	<b>90.00</b>	93.00	85.14	94.92	88.67	87.05	84.54
	ENS	<b>95.38</b>	89.53	<b>97.00</b>	89.82	<b>59.00</b>	<b>62.78</b>	76.53	86.67	<b>96.00</b>	<b>91.43</b>	<b>96.60</b>	<b>91.00</b>	89.92	<b>86.28</b>
Resnet50	MeLU (k=8)	94.46	89.30	94.20	92.18	54.00	61.86	75.73	89.17	97.00	88.57	95.60	87.67	88.71	85.26
MaxInput=255	MeLU (k=4)	92.92	90.23	95.00	91.82	57.00	59.79	<b>78.40</b>	87.50	97.33	85.14	95.72	89.33	88.26	85.26
	SReLU	92.31	89.42	93.00	90.73	56.50	59.69	73.33	<b>91.67</b>	<b>98.33</b>	88.95	95.52	89.67	87.88	85.15
	APLU	95.08	89.19	93.60	90.73	47.50	56.91	75.20	89.17	97.33	87.05	95.68	89.67	89.47	84.35
	ReLU	93.54	89.88	95.60	90.00	55.00	58.45	77.87	90.00	93.00	85.14	94.92	88.67	87.05	84.54
	ENS	93.85	91.28	96.20	<b>93.27</b>	59.00	63.30	77.60	<b>91.67</b>	98.00	87.43	96.30	89.00	89.17	86.62
eENS		<b>94.77</b>	<b>91.40</b>	<b>97.00</b>	92.91	<b>60.00</b>	<b>64.74</b>	77.87	88.75	98.00	<b>90.10</b>	<b>96.50</b>	<b>90.00</b>	<b>89.77</b>	<b>87.06</b>

Table 4. Performance obtained using Vgg16.

	Activation	CH	HE	LO	TR	RN	TB	LY	MA	LG	LA	CO	BG	LAR	Avg
Vgg16	MeLU (k=8)	<b>99.69</b>	92.09	98.00	92.91	59.00	60.93	78.67	87.92	<b>86.67</b>	93.14	95.20	89.67	90.53	86.49
MaxInput=1	Leaky ReLU	99.08	91.98	98.00	93.45	66.50	61.13	80.00	92.08	<b>86.67</b>	91.81	95.62	91.33	88.94	87.43
	ELU	98.77	<b>93.95</b>	97.00	92.36	56.00	59.69	81.60	90.83	78.33	85.90	95.78	93.00	90.45	85.66
	MeLU (k=4)	99.38	91.16	97.60	92.73	64.50	62.37	81.07	89.58	86.00	89.71	95.82	89.67	93.18	87.13
	PReLU	99.08	90.47	97.80	94.55	64.00	60.00	81.33	<b>92.92</b>	78.33	91.05	95.80	92.67	90.38	86.79
	SReLU	99.08	91.16	97.00	93.64	65.50	60.62	82.67	90.00	79.33	93.33	96.10	94.00	92.58	87.30
	APLU	99.08	92.33	97.60	91.82	63.50	62.27	77.33	90.00	82.00	92.38	96.00	91.33	90.98	86.66
	ReLU	<b>99.69</b>	93.60	98.20	93.27	<b>69.50</b>	61.44	80.80	85.00	85.33	88.57	95.50	93.00	91.44	87.33
	ENS	99.38	93.84	<b>98.40</b>	<b>95.64</b>	68.00	<b>65.67</b>	<b>85.07</b>	92.08	85.00	<b>96.38</b>	<b>96.74</b>	<b>94.33</b>	<b>92.65</b>	<b>89.47</b>
Vgg16	MeLU (k=8)	<b>99.69</b>	92.09	97.40	93.09	59.50	60.82	80.53	88.75	80.33	88.57	95.94	90.33	88.33	85.79
MaxInput=255	MeLU (k=4)	99.38	91.98	98.60	92.55	66.50	59.59	84.53	91.67	<b>88.00</b>	94.86	95.46	93.00	<b>93.03</b>	88.39
	SReLU	98.77	93.14	97.00	92.18	65.00	62.47	77.60	89.58	76.00	96.00	95.84	94.33	89.85	86.75
	APLU	98.77	92.91	97.40	93.09	63.00	57.32	82.67	90.42	77.00	90.67	94.90	93.00	91.21	86.33
	ReLU	<b>99.69</b>	93.60	98.20	93.27	<b>69.50</b>	61.44	80.80	85.00	85.33	88.57	95.50	93.00	91.44	87.33
	ENS	99.38	93.84	<b>98.80</b>	95.27	68.50	64.23	84.53	92.50	81.33	<b>96.57</b>	96.66	95.00	92.20	89.13
eENS		99.38	<b>94.07</b>	<b>98.80</b>	<b>95.64</b>	69.00	<b>65.88</b>	<b>85.87</b>	<b>93.33</b>	82.67	<b>96.57</b>	<b>96.88</b>	<b>95.33</b>	92.50	<b>89.68</b>

The protocol used in our experiments is a five-fold cross-validation, unless differently specified in the dataset description above. To validate the experiments the Wilcoxon signed rank test [24] has been used.

We substituted ReLU with a different activation function after every convolutional layer. In tables 3 and 4 we report the performance obtained using different activation functions coupled with Vgg16 and ResNet50. To reduce the computation time all the results are calculated using a batch size (BS) of 30 and a learning rate (LR) of 0.0001 for 30 epochs. As data augmentation we have

used a random reflection in both axis and two independent random rescales of both axis by two factors uniformly sampled in [1,2]. This means that the vertical and horizontal proportions of the new image are rescaled.

We have tested two ensembles:

- ENS, sum rule among all the methods with a given MaxInput of a given CNN;
- eENS, sum rule among all the methods of a given CNN.

In Table 5 we report performance, in some datasets, obtained choosing optimal values of BS and LR for ReLU. Also with BS and LR optimized for ReLU the performance of ENS is higher than that obtained by ReLU.

Table 5. Performance with optimized BS and LR.

	Activation	CH	LA		MA
Resnet50	MeLU (k=8)	98.15	98.48	Vgg16	90.42
MaxInput=255	MeLU (k=4)	98.15	98.67	MaxInput=255	87.08
BS=10				BS=50	
LR=0.001	SReLU	99.08	96.00	LR=0.0001	88.33
	APLU	98.46	98.48		93.75
	ReLU	97.23	96.57		92.08
	ENS	<b>99.38</b>	<b>99.05</b>		<b>93.75</b>

From the results reported in Tables 3, 4 & 5 the following conclusions can be drawn:

- both ENS and eENS outperform with a p-value of 0.05 all the stand-alone activation functions. Moreover, eENS outperforms ENS in both the CNN topologies (i.e. Vgg16 and ResNet50) with a p-value of 0.05. This is the most important finding of this work;
- MeLU obtains the best average performance in both the CNNs;
- Different behavior occurs in the two topologies, in ResNet50 there is a clear performance difference between  $MaxInput = 1,255$ , while in Vgg16 similar performance is obtained with  $MaxInput = 1,255$ .
- Also optimizing BS and LR for ReLU similar conclusions are obtained, ENS outperforms other activation functions, including ReLU.

## Conclusion

The purpose of the present paper was to evaluate the performance of an ensemble of CNNs created by changing the activation functions in famous pre-trained networks. Besides, we tested several activation functions on several challenging datasets and reported their results. We also proposed a new activation function called Mexican Linear Unit.

Our experiments show that an ensemble of multiple CNNs that only differ in the activation functions outperforms the results of the single CNNs. Besides, we show that there is not an activation that is consistently better than the others. In particular, we see that MeLU is competitive with the other activation functions in the literature. MeLU also seems to be the best performing activation when  $k = 4$ , in particular on VGG16. Notice that we only tested MeLU with  $k = 4,8$ , we did not cherry-picked the best performing parameters  $k$  on the test set. As future work we aim to create even larger ensembles of CNNs to see how much we can boost the performances of the single CNNs. The drawbacks of this approach are speed and memory requirements. However, we plan to do it with very small CNNs and see if such an ensemble is competitive with much larger networks which are still larger than the ensemble. Finally, we share the MATLAB code of every activation and ensemble that we created.

## Acknowledgment

We gratefully acknowledge the support of NVIDIA Corporation for the “NVIDIA Hardware Donation Grant” of a Titan X used in this research.

## 5. Bibliography

[1] K. He, X. Zhang, S. Ren, J. Sun, Deep Residual Learning for Image Recognition, 2016 IEEE Conf. Comput. Vis. Pattern Recognit. (2016) 770–778.

[2] S. Ren, K. He, R.B. Girshick, J. Sun, Faster R-CNN: Towards Real-Time Object Detection with Region Proposal Networks, IEEE Trans. Pattern Anal. Mach. Intell. 39 (2015) 1137–1149.

[3] F. Schroff, D. Kalenichenko, J. Philbin, FaceNet: A unified embedding for face recognition and clustering, 2015 IEEE Conf. Comput. Vis. Pattern Recognit. (2015) 815–823.

[4] D. Bahdanau, K. Cho, Y. Bengio, Neural Machine Translation by Jointly Learning to Align and Translate, CoRR. abs/1409.0 (2015).

[5] X. Glorot, A. Bordes, Y. Bengio, Deep Sparse Rectifier Neural Networks, in: AISTATS, 2011.

[6] V. Nair, G.E. Hinton, Rectified Linear Units Improve Restricted Boltzmann Machines, in: ICML, 2010.

[7] A. Krizhevsky, I. Sutskever, G.E. Hinton, ImageNet Classification with Deep Convolutional Neural Networks, Commun. ACM. 60 (2012) 84–90.

[8] A.L. Maas, Rectifier Nonlinearities Improve Neural Network Acoustic Models, in: 2013.

[9] D.-A. Clevert, T. Unterthiner, S. Hochreiter, Fast and Accurate Deep Network Learning by Exponential Linear Units (ELUs), CoRR. abs/1511.0 (2015).

[10] G. Klambauer, T. Unterthiner, A. Mayr, S. Hochreiter, Self-Normalizing Neural Networks, in: NIPS, 2017.

[11] K. He, X. Zhang, S. Ren, J. Sun, Delving Deep into Rectifiers: Surpassing Human-Level Performance on ImageNet Classification, 2015 IEEE Int. Conf. Comput. Vis. (2015) 1026–1034.

[12] F. Agostinelli, M.D. Hoffman, P.J. Sadowski, P. Baldi, Learning Activation Functions to Improve Deep Neural Networks, CoRR. abs/1412.6 (2014).

[13] S. Scardapane, S. Van Vaerenbergh, A. Uncini, Kafnets: kernel-based non-parametric activation functions for neural networks, Neural Netw. 110 (2018) 19–32.

[14] F. Manessi, A. Rozza, Learning Combinations of Activation Functions, 2018 24th Int. Conf. Pattern Recognit. (2018) 61–66.

[15] P. Ramachandran, B. Zoph, Q. V Le, Searching for Activation Functions, CoRR. abs/1710.0 (2017).

[16] K. Simonyan, A. Zisserman, Very Deep Convolutional Networks for Large-Scale Image Recognition, CoRR. abs/1409.1 (2015).

[17] X. Jin, C. Xu, J. Feng, Y. Wei, J. Xiong, S. Yan, Deep Learning with S-shaped Rectified Linear Activation Units, in: AAAI, 2016.

[18] M. V Boland, R.F. Murphy, A neural network classifier capable of recognizing the patterns of all major subcellular structures in fluorescence microscope images of HeLa cells, Bioinformatics. 17

12 (2001) 1213–1223.

- [19] S. Moccia, E. De Momi, M. Guarnaschelli, M. Savazzi, A. Laborai, L. Guastini, G. Peretti, L.S. Mattos, M. V Boland, R.F. Murphy, N.A. Hamilton, R.S. Pantelic, K. Hanson, R.D. Teasdale, Fast automated cell phenotype image classification, *Bioinformatics*. 17 12 (2001) 1213–1223. doi:10.1186/1471-2105-8-110.
- [20] L. Shamir, N. Orlov, D.M. Eckley, T.J. Macura, I.G. Goldberg, IICBU 2008: a proposed benchmark suite for biological image analysis, *Med. Biol. Eng. Comput.* 46 (2008) 943–947.
- [21] J.N. Kather, C.A. Weis, F. Bianconi, S.M. Melchers, L.R. Schad, T. Gaiser, A. Marx, F.G. Zöllner, Multi-class texture analysis in colorectal cancer histology, in: *Sci. Rep.*, 2016.
- [22] K. Dimitropoulos, P. Barmpoutis, C. Zioga, A.I. Kamas, K. Patsiaoura, N. Grammalidis, Grading of invasive breast carcinoma through Grassmannian VLAD encoding, in: *PLoS One*, 2017.
- [23] S. Moccia, E. De Momi, M. Guarnaschelli, M. Savazzi, A. Laborai, L. Guastini, G. Peretti, L.S. Mattos, Confident texture-based laryngeal tissue classification for early stage diagnosis support, *J. Med. Imaging*. 4 (2017) 34502.
- [24] J. Demsar, Statistical Comparisons of Classifiers over Multiple Data Sets, *J. Mach. Learn. Res.* 7 (2006) 1–30.